Karirat T *et al.* (2025)
Notulae Botanicae Horti Agrobotanici Cluj-Napoca
Volume 53, Issue 1, Article number 14149
DOI:10.15835/nbha53114149
Research Article

Impact of non-thermal plasma seed priming and early development stages of two local Thai Cruciferous plants mustard green and rat-tailed radish on glucosinolates, isothiocyanates, minerals, antioxidant and anticancer activities

Thipphiya KARIRAT[1], Worachot SAENGHA[1], Khanit MATRA[2], Kannika NAKHOWONG[1], Pimsupa PATTANU[1], Piyatida KITKAYUN[1], Theerayut BUBPAMALA[1], Benjaporn BURANRAT[3], Sirirat DEESEENTHUM[1], Teeraporn KATISART[4], Vijitra LUANG-IN[1]*

[1]*Mahasarakham University, Faculty of Technology, Department of Biotechnology, Natural Antioxidant Innovation Research Unit, Maha Sarakham 44150, Thailand; thipphiya.k@gmail.com; worachot207@gmail.com; N.kannika4700@gmail.com; pattanu.p@outlook.com; piyatida.2341@gmail.com; theerayut.b@kkumail.com; sirirat.d@msu.ac.th; vijitra.l@msu.ac.th (*corresponding author)*
[2]*Srinakharinwirot University, Faculty of Engineering, Department of Electrical Engineering, Nakhon Nayok 26120, Thailand; khanit@g.swu.ac.th*
[3]*Mahasarakham University, Faculty of Medicine, Mahasarakham 44000, Thailand; benjaporn.b@msu.ac.th*
[4]*Mahasarakham University, Faculty of Science, Department of Biology, Maha Sarakham 44150, Thailand; teeraporn@msu.ac.th*

Abstract

Over the past decade, non-thermal plasma (NTP) technology has emerged as a promising tool in the food sector. Cruciferous microgreens are known for their anticancer properties, yet the potential of certain varieties at early developmental stages remains underexplored. This study investigated the effects of NTP treatment on seed priming and plant development at 14, 21, and 28 days in mustard green (MG) (*Brassica juncea* (L.) Czern) and rat-tailed radish (RTR) (*Raphanus sativus* var. *caudatus*), focusing on their bioactive compounds and bioactivities. NTP treatment significantly affects stem length, fresh weight, or dry weight compared to untreated seeds. It also enhanced the production of glucosinolates, isothiocyanates (ITCs), specific minerals, total phenolics, total flavonoids, and biological activities in both plants. MG was found to contain sinigrin, gluconapin, allyl ITC, and 3-butenyl ITC, while RTR contained glucoraphasatin and raphasatin. MG exhibited IC_{50} values ranging from 16–78 μg/mL in cytotoxicity tests against four cancer cell lines HeLa, HepG2, MCF-7 and HT-29 with enhanced activity from NTP. RTR demonstrated greater effectiveness with IC_{50} values of 12–60 μg/mL with higher activity from NTP. Both plant extracts especially NTP-treated samples reduced cancer cell survival and proliferation by upregulating pro-apoptotic genes (*Bax*, *caspase-3*, and *p21*) and proteins while downregulating anti-apoptotic and metastatic markers (*Bcl-2*, *MMP-9*, *MMP-2*, and *cyclin D1*). NTP can enhance the therapeutic bioactivity of young plants, with both MG and RTR at 14 and 21 days of growth, showing the higher potential for anticancer applications.

Received: 27 Sep 2024. Received in revised form: 26 Dec 2024. Accepted: 21 Jan 2025. Published online: 26 Feb 2025.
From Volume 49, Issue 1, 2021, Notulae Botanicae Horti Agrobotanici Cluj-Napoca journal uses article numbers in place of the traditional method of continuous pagination through the volume. The journal will continue to appear quarterly, as before, with four annual numbers.

Keywords: apoptosis; allyl isothiocyanates; *Brassica juncea*; 3-butenyl isothiocyanates; *Raphanus sativus*; raphasatin

Introduction

The agricultural sector faces growing challenges in meeting the dual objectives of improving crop productivity and nutritional quality while maintaining environmental sustainability. Among the innovative strategies addressing these challenges, non-thermal plasma (NTP) technology has emerged as a promising tool. NTP, characterized by reactive species, ions, and electrons, offers a sustainable and energy-efficient method for seed priming. By inducing oxidative stress, NTP treatment has been shown to enhance seed germination, plant growth, and bioactive compound synthesis, resulting in improved phytochemical profiles across diverse species (Matra, 2018; Saengha *et al*., 2021; Tanakaran and Matra, 2022; Bhabani *et al*., 2024; Jia *et al*., 2024).

Cruciferous vegetables are renowned for their health-promoting properties, rich in bioactive compounds such as glucosinolates (GSLs) and their hydrolysis products, including isothiocyanates (ITCs), which exhibit potent antioxidant and anticancer activities (Zeng *et al*., 2023). Glucosinolates, sulfur-containing secondary metabolites, are hydrolyzed by the enzyme myrosinase upon cellular disruption, producing bioactive compounds such as ITCs, indoles, and nitriles (Verkerk *et al*., 2009). Among these, ITCs have garnered particular attention for their ability to modulate carcinogenesis by inducing phase II detoxification enzymes, inhibiting tumor cell proliferation, and promoting apoptosis (Nandini *et al*., 2020). Despite their well-documented benefits, the content and bioactivity of GSLs and ITCs are influenced by genetic, environmental, and agronomic factors (Blažević *et al*., 2020).

In Thailand, Cruciferous vegetables such as mustard green (MG) (*Brassica juncea* (L.) Czern) and rat-tailed radish (RTR) (*Raphanus sativus* var. *caudatus*) hold significant potential as sources of bioactive compounds (Saengha *et al*., 2021; Luang-In *et al*., 2021). Recent studies have shown that seed priming with NTP enhances the total ITC content and anticancer activity of these plants, particularly in 7-day-old microgreens, which exhibit efficacy against liver (HepG2) and breast (MCF-7) cancer cell lines (Saengha *et al*., 2021; Luang-In *et al*., 2021). However, the bioactive and nutritional potential of these plants at later developmental stages, such as 14, 21, and 28 days, remains underexplored. These stages, often overlooked due to lower fresh weight compared to mature plants, may hold untapped potential in terms of GSLs, ITCs, minerals, antioxidants, and anticancer activities.

Cancer remains a leading global cause of mortality, accounting for 9.3 million deaths annually, representing 22.7% of all non-communicable disease-related deaths (Ferlay *et al*., 2024). In Thailand, the burden of cancer is considerable, with 183,541 new cases and 118,829 deaths reported in 2022. Liver, lung, and colorectal cancers are the most prevalent among males, while breast, liver, and cervical cancers dominate among females (Ferlay *et al*., 2024). Epidemiological studies have linked the consumption of cruciferous vegetables to reduced cancer risk, as evidenced by systematic reviews and meta-analyses. For instance, Li *et al*. (2022) highlighted that cruciferous vegetable intake is associated with a reduced risk of gastric and lung cancers. Similarly, Morrison *et al.* (2019) found an inverse relationship between cruciferous vegetable consumption and gastric cancer risk. These findings underscore the critical role of GSLs and ITCs in cancer prevention, achieved through mechanisms such as detoxification enzyme modulation and oxidative stress reduction (Fujioka *et al*., 2016; Wang *et al*., 2015).

In addition to phytochemicals, the mineral composition of plants is essential for their nutritional (Sarkar *et al*., 2023; Mir *et al*., 2017). MG plants are rich in essential minerals such as calcium, magnesium, potassium, and iron, which are crucial for maintaining human health. These minerals are vital for various physiological functions, including bone health, enzymatic reactions, and cardiovascular function (Tunsagool *et al*., 2023).

Understanding how NTP seed priming influences these mineral profiles provides valuable insights into the broader metabolic impacts of this technology.

This study aims to evaluate the effects of NTP seed priming on MG and RTR, focusing on glucosinolate and isothiocyanate content, mineral composition, antioxidant capacity, and anticancer activities across different developmental stages. By elucidating the biochemical and physiological changes induced by NTP treatment, this research seeks to enhance the value of these underutilized crops and promote their application in sustainable agriculture and functional food development. The findings of this study align with Thailand's Bio-Circular-Green (BCG) economic model, emphasizing innovation-driven growth in agriculture and biotechnology. By demonstrating the potential of NTP technology to improve the nutritional and therapeutic qualities of local cruciferous plants, this research contributes to the broader efforts to address global food security and public health challenges.

Materials and Methods

Plant cultivation, NTP conditions and plant extraction

MG and RTR seeds were sourced from Punthawee Mall Shop (*https://www.pwcmallonline.com*). Following the protocol described in previous studies (Luang-In *et al.*, 2021; Saengha *et al.*, 2021), MG and RTR seeds (100 seeds per replicate per treatment) were treated in triplicate with NTP. The voltage was set at 21 kV for MG and 19 kV for RTR, with a treatment duration of 5 min. The average discharge currents for these two conditions were around 0.51 and 0.32 mA, while the discharge voltages were around 11.02, and 10.93 kV, respectively. The experiments were conducted at the Faculty of Engineering, Srinakharinwirot University, Nakhon Nayok Province. The seeds were sprayed daily with 20 mL of deionized water and germinated in trays under controlled conditions: 25 °C with a 12-h light/12-h dark cycle and a light intensity of 42 μmol/s/m^2. Harvesting occurred at three time points: 14, 21, and 28 days. At harvest, plants were cut 1 cm above the vermiculite surface for further analysis. Plants grown from plasma-treated seeds were labelled as RTR-P and MG-P, while those grown from untreated seeds were labeled as RTR-C and MG-C. Measurements including stem length, fresh weight, and dry weight were recorded. For further analysis, freeze-dried plants (10 g) were homogenized in 500 mL of 80% methanol and incubated at 37 °C with constant shaking at 250 rpm for 24 h. The homogenates were centrifuged at 10,000 × g for 15 min, and the supernatants were filtered. The resulting extracts were freeze-dried and reconstituted in ethanol to prepare stock solutions with a concentration of 20 mg/mL, which were subsequently used for antioxidant assays.

Scanning electron microscopy (SEM)

The surface morphology of untreated and plasma-treated seeds was analyzed using Scanning Electron Microscopy (SEM). Prior to imaging, the seeds were coated with a 30 nm layer of gold to enhance conductivity. Observations were conducted using a Leo/1450 SEM (Carl Zeiss, Germany) at an accelerating voltage of 5 kV.

2,2-diphenyl-1-picrylhydrazyl (DPPH) radical scavenging activity

The electron or hydrogen atom donation ability of the extracts was evaluated by decolorizing a purple methanol solution of the stable DPPH free radical, following the method outlined in a previous study (Karirat *et al.*, 2024). For the assay, 20 μL of 20 mg/mL extract was combined with 180 μL of 10 mM DPPH• solution (prepared in ethanol) (Sigma-Aldrich, St. Louis, MO, USA). After a 30-min incubation period, the absorbance at 515 nm was measured using a M965+ microplate reader (Metertech, Taipei, Taiwan). A Trolox standard curve was generated to express the DPPH scavenging activity in terms of mg Trolox Equivalent (TE) per gram of extract, with all measurements performed in triplicate.

2,2'-azino-bis(3-ethylbenzothiazoline-6-sulfonic acid (ABTS) radical scavenging activity

The ABTS cation radical was generated by dissolving 10 mg of ABTS and 2 mg of potassium persulfate in water, following the procedure described by Seeram *et al.* (2006). The mixture was left in the dark at room temperature for 12-16 h to allow for full reaction. Prior to use, 1 mL of the prepared ABTS solution was diluted with 60 mL of methanol. For the assay, 20 µL of 20 mg/mL extract was combined with 180 µL of ABTS solution in triplicates and incubated for 30 min. The percentage of inhibition of absorbance at 734 nm was calculated using the formula stated below: A Trolox standard curve was generated to express the ABTS scavenging activity in terms of mg Trolox Equivalent (TE) per gram of extract, with all measurements performed in triplicate.

Total phenolic content (TPC) and total flavonoid content (TFC)

The total phenolic content (TPC) was determined using the Folin-Ciocalteu reagent, following the method described in a previous study (Karirat *et al.*, 2024). The reaction mixture contained 100 µL of a 10% Folin-Ciocalteu solution, 20 µL of the extract (20 mg/mL), and 80 µL of 7.35% sodium carbonate. After incubating the mixture at room temperature for 30 min, the absorbance was measured at 725 nm using a M965+ microplate reader (Metertech, Taipei, Taiwan). TPC was expressed as milligrams of gallic acid equivalent (GAE) per gram of extract. The total flavonoid content (TFC) was quantified using a colorimetric method (Karirat *et al.*, 2024). The reaction mixture consisted of 60 µL of deionized water, 20 µL of the extract (20 mg/mL), 10 µL of 10% aluminum trichloride, and 10 µL of 5% sodium nitrate. After a 30-min reaction, 100 µL of 1 M sodium hydroxide was added, and the absorbance was recorded at 420 nm. Results were expressed as milligrams of rutin equivalent (RE) per gram of extract, with all measurements performed in triplicate.

Total ITC content by spectrophotometric assay

Microgreens harvested at 14, 21, and 28 days were freeze-dried following the method outlined by Saengha *et al*. (2021). A 250 mg portion of the dried samples was combined with 4 mL of 0.1 M citrate–phosphate buffer (pH 7.0) and incubated at 37 °C in a shaking incubator at 250 rpm for 1 h. The resulting extract was then mixed with dichloromethane (DCM) in a 1:1 ratio and further incubated at 37 °C at 250 rpm for 30 min. Following this, the samples were centrifuged at 10,000 × g for 15 min. The DCM phase (lower layer) was collected and treated with 0.5 g of $MgSO_4$ to remove water. The supernatant was diluted with methanol at a 1:4 ratio, dried using a rotary evaporator at 40 °C, and redissolved in 10 µL of methanol to quantify the total isothiocyanate (ITC) content. For the ITC analysis, 10 µL of the extract was added to a 96-well plate with 90 µL of methanol, 90 µL of 0.1 M phosphate buffer (pH 8.0), and 10 µL of 0.08 M 1,3-benzodithiole-2-thione. The mixture was incubated at 60 °C for 2 h, and absorbance at 365 nm was measured using a microplate reader (M965+; Metertech Inc., Taipei, Taiwan). Allyl isothiocyanate (AITC) from Sigma-Aldrich (Poole, UK) was used as the ITC standard.

GC-MS analysis for ITC quantification

For GC-MS analysis, freeze-dried samples (500 mg) were extracted with 3 mL of DCM in sealed test tubes, shaken for 24 h at 250 rpm at room temperature. After centrifugation at 16,100 × g for 5 min, 1 mL of the supernatant was treated with 0.5 g magnesium sulfate, mixed, and centrifuged again for 20 min. The clear supernatant was transferred to vials for GC-MS analysis. ITC analysis was performed using a Shimadzu QP2010 system with an Agilent HP-5MS capillary column, under conditions previously described (Saengha *et al*., 2021). ITCs were identified using the GC-MS mass spectral library and quantified using standard curve of AITC standard.

Glucosinolate quantification by HPLC analysis

The method for GSL extraction was adapted from Luang-In *et al.* (2018) with minor adjustments. Freeze-dried samples (5 g) were ground and mixed with 5 mL of 70% methanol, shaken at 37 °C for 5 min, and centrifuged at 8,000 × g for 15 min. The remaining solids were re-extracted, and the supernatants from both extractions were combined, dried in an oven at 70 °C, and dissolved in 1 mL of deionized water using a vortex mixer. The 1 mL sample was processed through DEAE-25A anion exchange resin as described by Luang-In *et al*. (2014). GSL analysis was conducted using an HPLC-DAD system (Shimadzu, Kyoto, Japan) equipped with a Synergi 4 µm Hydro-RP 80A column (150 × 2 mm, 4.6 µm, Phenomenex Inc., Torrance, CA, USA) and a security guard column AQ C18 (4 × 3 mm). The system included Shimadzu LC-20AC pumps and an SPD-M20A diode array detector. A gradient of Solvent A (water) and Solvent B (acetonitrile) was applied as follows: 2% B for 15 min, 2-25% B over 2 min, 25-70% B over 2 min, 70% B hold for 2 min, 70-2% B over 2 min, and 2% B for 15 min, at a flow rate of 0.2 mL/min at 35 °C. Eluents were monitored at 229 nm. Desulfoglucosinolate (DS-GSL) quantification was performed using response factors for each GSL relative to the external standard sinigrin, with pure sinigrin sourced from Sigma-Aldrich Co. (St. Louis, MO, USA).

Nutrient and mineral content analysis

All samples were dried at 60°C, ground to fine powder, and digested prior to analysis. The total nitrogen content (%) of the samples was determined using the combustion method, utilizing a multi EA 4000 elemental analyzer (Analytik Jena AG, Germany). Phosphorus content (%) was measured using the vanadomolybdate method, a colorimetric technique. The powdered sample was digested in an acidic medium, and the phosphorus was reacted with ammonium molybdate and ammonium vanadate to produce a yellow complex. Absorbance was measured spectrophotometrically at 400 nm to quantify phosphorus concentration. Mineral analysis (Calcium, Magnesium, Potassium, Sodium, Iron, Manganese, Copper, and Zinc) was quantified using Atomic Absorption Spectroscopy (AAS) (PerkinElmer, USA). Sample preparation involved digestion with concentrated nitric acid in a microwave digestion system. The digested samples were diluted and analyzed for the following minerals: Calcium (Ca), Magnesium (Mg), Potassium (K), and Sodium (Na) were measured in percentage concentrations (%). Iron (Fe) and Copper (Cu) were quantified in milligrams per kilogram (mg/kg). Manganese (Mn) and Zinc (Zn) were expressed as percentage concentrations (%). Total sulfur content (%) was determined using the combustion method on the multi-EA 4000 elemental analyzer. The heatmaps of nutrient and mineral content analysis were created by GraphPad Prism 9.0 (Boston, MA, USA).

Cancer cell cultivation

Four cancer cell lines, MCF-7, HepG2, HeLa, and HT-29, were sourced from the American Type Culture Collection (Manassas, VA, USA). The cells were cultured in Dulbecco's Modified Eagle Medium (DMEM) supplemented with 10% fetal bovine serum, 100 U/mL penicillin, and 100 µg/mL streptomycin (Invitrogen, Carlsbad, CA, USA) at 37 °C in a 5% CO_2 atmosphere. The culture medium was refreshed every 2-3 days. For maintenance, the cells were washed with phosphate-buffered saline (PBS, pH 7.2) and detached using 0.25% Trypsin-EDTA (Invitrogen, Carlsbad, CA, USA).

Plant extraction for cell cultures

Plant extraction was performed as described by Luang-In *et al*. (2021). Fresh plants (50 g) were ground and mixed with 50 mL of 0.1 M citrate-phosphate buffer (pH 7.0) at 37 °C, shaking at 250 rpm for 2 h. DCM was added in a 1:1 ratio, and the mixtures were agitated for 30 min, followed by centrifugation at 10,000 × g for 15 min. The supernatants were filtered, evaporated, and freeze-dried. The dried extracts were dissolved in 1% dimethyl sulfoxide (DMSO) (Fisher Scientific, Loughborough, UK) at a concentration of 1,000 µg/mL. The solutions were filtered using a 0.22 µm syringe filter for sterility. For the MTT assay, serial dilutions of the

extracts were prepared in DMEM at concentrations of 3.91, 7.81, 15.6, 31.3, 62.5, 125, and 250 µg/mL. For other assays, appropriate serial dilutions were prepared similarly from the stock solution.

Cytotoxicity assay

Cancer cells (5×10^3 cells/mL) were seeded in 96-well plates and incubated for 24 h at 37 °C in a 5% CO_2 atmosphere. The cells were treated with plant extracts at concentrations ranging from 0 to 250 µg/mL for 24, 48, and 72 h. After treatment, 0.5 mg/mL of 3-(4,5-dimethylthiazol-2-yl)-2,5-diphenyltetrazolium bromide (MTT) was added to each well and incubated for 4 h. The MTT solution was then removed and replaced with 200 µL of DMSO to solubilize the MTT formazan crystals. This assay evaluates mitochondrial function, as the mitochondrial dehydrogenase enzyme in living cells converts the yellow MTT tetrazolium salt into purple MTT formazan. The absorbance was recorded at 590 nm to assess cell viability. The maximum cytotoxicity (*E*max) and the half-maximal inhibitory concentration (IC_{50}) values were determined.

$$Emax = \frac{(\text{Acontrol} - \text{Asample})}{(\text{Acontrol})} \times 100$$

An IC_{50} value below 50 µg/mL signifies high cytotoxicity. IC_{50} values between 50–100 µg/mL indicate moderate cytotoxicity, while values of 100–200 µg/mL and 200–300 µg/mL represent weak and extremely weak cytotoxicity, respectively.

Clonogenic assay

A colony formation assay was performed to evaluate the effects of plant extracts on cancer cell growth (Saengha *et al*., 2024). Viable cancer cells (800 cells/well) were seeded into 6-well plates and treated with plant extracts at concentrations of 0, 6.25, 12.5, 25, 50, and 100 µg/mL for 24 h. Following treatment, the cells were washed with PBS and cultured in fresh DMEM for 14 days. After the incubation period, the medium was removed, and the cells were washed, fixed, and stained with 0.5% crystal violet for 1 h. The stained colonies were rinsed and photographed using a Nikon D50 digital camera.

Migration wound healing assay

Cancer cells at 100% confluency were subjected to scratch wound markings and subsequently rinsed with PBS. The cells were then treated with plant extract (50 µg/mL) and allowed to migrate for 24 and 48 h. Wound closure was observed under an inverted microscope, and the percentage of wound coverage was calculated using the formula:

$$\text{Relative wound coverage (\%)} = \frac{(\text{initial wound area} - \text{final wound area})}{(\text{initial wound area})} \times 100$$

Real-time polymerase chain reaction (real-time PCR) analysis

Real-time PCR was conducted to analyze changes in apoptotic and migration-related mRNA expression following 24-h treatment with MG and RTR extracts. Cancer cells (2×10^5 cells/well) were cultured in 6-well plates at 37 °C for 24 h before being treated with plant extracts (50 µg/mL) under the same conditions. Total RNA was extracted using TRIzol™ reagent (Thermo Fisher Scientific, IL, USA) and converted to cDNA using iScript™ Reverse Transcription Supermix (Bio-Rad, Hercules, CA, USA). Quantitative RT-PCR was performed using the Fast Start Essential DNA Green Master (Roche Applied Science) on a QuantStudio real-time PCR system (Applied Biosystems, Foster City, CA, USA). Primers targeting *Bax, Bcl2, caspase-3, p21, MMP-2, MMP-9*, and *cyclin D1* were used (Table 1), with GAPDH serving as the reference gene. PCR conditions were set to 94 °C for 10 min (denaturation), 60 °C for 10 s (annealing), and 72 °C (extension) for 10 cycles.

Table 1. Primers for real-time PCR analysis

Gene	Primer	Sequence (5'->3')	Size (bp)
GAPDH	Forward	CACTGCCAACGTGTCAGTGGTG	121
	Reverse	GTAGCCCAGGATGCCCTTGAG	
Bax	Forward	TGCTTCAGGGTTTCATCCAG	170
	Reverse	GGCGGCAATCATCCTCTG	
Bcl2	Forward	AGGAAGTGAACATTTCGGTGAC	149
	Reverse	GCTCAGTTCCAGGACCAGGC	
caspase-3	Forward	GGCGCTCTGGTTTTCGTTAAT	121
	Reverse	TCCAGAGTCCATTGATTCGCT	
p21	Forward	AGTCAGTTCCTTGTGGAGCC	109
	Reverse	GCATGGGTTCTGACGGACAT	
MMP-2	Forward	TTGACGGTAAGGACGGACTC	153
	Reverse	ACTTGCAGTACTCCCCATCG	
MMP-9	Forward	TTTGACAGCGACAAGAAGTG	208
	Reverse	CAGGGCGAGGACCATAGAGG	
cyclin D1	Forward	ATCTCTGTACTTTGCTTGCT	564
	Reverse	AGTACATGGATATTCCCAAA	

Protein extraction and Western blot analysis

Western blot analysis was performed to evaluate changes in apoptotic and migration-related proteins after 24-h treatment with MG and RTR extracts. Cancer cells were cultured in 6-well plates and treated with plant extracts (50 μg/mL) for 24 h. The cells were lysed on ice for 30 min using RIPA buffer (50 mM Tris-Cl pH 7.4, 150 mM NaCl, 1% NP-40, 0.5% sodium deoxycholate, 0.1% SDS) supplemented with a protease and phosphatase inhibitor cocktail (Roche, Penzberg, Germany). After centrifugation at 14,000 × g for 15 min at 4 °C, the protein content in the supernatant was quantified using a BCA protein assay kit (Thermo Fisher Scientific, IL, USA). A 25-μg protein sample was resolved by SDS-PAGE using a 12% polyacrylamide gel (Amersham Pharmacia Biotech, Piscataway, NJ, USA) and transferred to a nitrocellulose membrane. The membrane was blocked for 1 h at room temperature with Tris-buffered saline containing 0.1% Tween-20 (TBST) and incubated with primary antibodies (Boster Biological Technology, Inc., Wuhan, China). Following three washes with TBST, the membranes were incubated for 1 h with goat anti-rabbit or goat anti-mouse secondary antibodies conjugated to horseradish peroxidase (1:5000). Chemiluminescent detection was performed using Amersham ECL Prime, and protein band densities were visualized and quantified using MageQuant TL 400. β-actin was used as a housekeeping protein control, and all experiments were conducted in triplicate.

Statistical analysis

Data were expressed as mean ± standard deviation (SD) from three independent experiments. Statistical analysis was performed using SPSS (demo version), employing one-way analysis of variance (ANOVA) followed by Duncan's multiple range test. A p-value of < 0.05 was considered statistically significant.

Results

Seed morpholoical changes and plant growth

Under SEM analysis, the seed coat structure of MG seeds (60×, 100×, and 250× magnifications) is displayed before and after soaking for 12 h (Figure 1A).

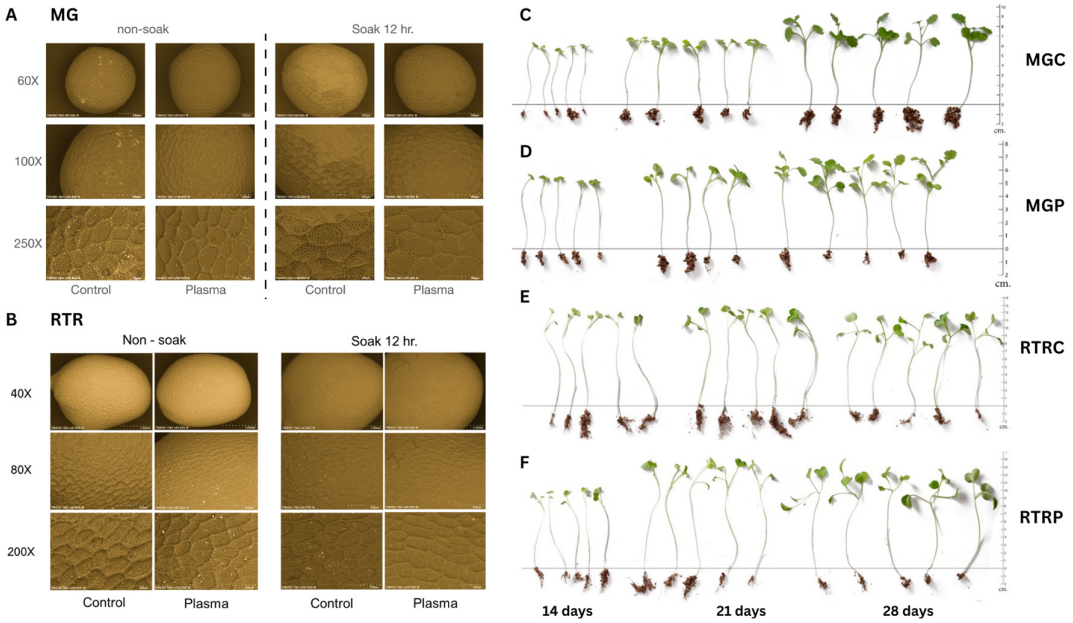

Figure 1. Seed morphological changes and plant growth
(A) Mustard green (MG) seeds from control and plasma-treated groups in non-soaked and soaked with water for 12 h. (B) Rat-tailed radish (RTR) seeds from control and plasma-treated groups in non-soaked and soaked with water for 12 h. (C) MG microgreen growth of control group (MGC) at 14, 21 and 28 days. (D) MG microgreen growth of plasma-treated group (MGP) at 14, 21 and 28 days. (E) RTR microgreen growth of control group (RTRC) at 14, 21 and 28 days. (F) RTR microgreen growth of plasma-treated group (RTRP) at 14, 21 and 28 days.

In the non-soaked condition, both control and plasma-treated seeds appear similar. However, after 12 h of soaking, in the control sample, the surface exhibited a highly porous structure with clearly defined pits and irregular cell boundaries. In contrast, the plasma-treated sample displayed a smoother surface with reduced porosity and fewer visible openings. These surface changes suggest that plasma treatment may enhance water absorption. Similarly, SEM images (40×, 80×, and 200× magnifications) reveal differences in RTR seed coats before and after soaking (Figure 1B). In non-soaked seeds, both control and plasma-treated seeds look indifferent. After soaking for 12 h, the control sample shows a rough surface with irregularly shaped and uneven cell boundaries, along with visible textural details. In contrast, the plasma-treated sample exhibits a smoother surface with more defined and compact cell boundaries, indicating a reduction in surface irregularities.

The growth performance of MG and RTR microgreens was observed over 14, 21, and 28 days. Plasma treatment may suppress the growth of MGC (Figure 1D) when compared to the control (Figure 1C). However, plasma-treated RTRP plants (Figure 1F) exhibit visibly enhanced growth, particularly noticeable after 21 and 28 days, when compared to the control (Figure 1E).

Physical and biological attributes

Table 2 presents the physical and biological attributes of MG microgreens under control and plasma-treated conditions at three different time points (14, 21, and 28 days).

As for physical aspects, the length of stem was significantly influenced by both the treatment type and the growth stage ($p < 0.05$). Plasma-treated microgreens had shorter stem lengths at 14 days (5.57±0.31 cm) compared to the control (6.13±0.43 cm). However, by 28 days, plasma-treated samples (7.67±0.28 cm) still exhibited shorter stems than the control group (9.12±0.33 cm). The fresh weight of early staged plants increased with time for both treatments. Plasma-treated microgreens at 28 days had the highest fresh weight (92.33±5.45 mg), which was comparable to the control (88.78±2.19 mg) but statistically significant (p =

0.001). A similar trend was observed for dry weight, with plasma-treated samples showing higher values than the control, particularly.

Table 2. Physical and biological attributes of MG

Parameter	Mustard green (MG)						Sig. ($p < 0.05$)
	Control 14d	Control 21d	Control 28d	Plasma 14d	Plasma 21d	Plasma 28d	
Physical aspects							
Length of stem (cm/microgreen)	6.13±0.43^{d}	6.55±0.24^{c}	9.12±0.33^{a}	5.57±0.31^{e}	6.64±0.28^{c}	7.67±0.28^{c}	0.000
Fresh weight (mg/microgreen)	64.42±8.54^{c}	84.20±5.52^{ab}	88.78±2.19^{a}	75.10±8.72^{b}	85.66±0.00^{ab}	92.33±5.45^{a}	0.001
Dry weight (mg/microgreen)	2.50±1.53^{b}	3.02±0.00^{b}	3.82±0.07^{ab}	3.07±0.19^{b}	5.29±2.00^{a}	5.26±0.30^{a}	0.023
Bioactive compounds							
Sinigrin (µmol/g DW)	16.61±0.84^{c}	19.52±0.24^{b}	12.27±1.64^{d}	22.71±2.20^{a}	20.61±0.85^{ab}	10.87±1.05^{d}	0.000
Gluconapin (µmol/g DW)	33.14±2.00^{c}	30.19±3.16^{c}	15.36±0.79^{d}	41.81±2.10^{a}	37.53±2.36^{ab}	4.63±0.82^{e}	0.000
AITC (µmol/g DW)	5.73±0.02^{d}	6.71±0.11^{c}	4.97±0.05^{e}	8.30±0.21^{a}	8.05±0.26^{a}	7.19±0.10^{b}	0.000
3-Butenyl ITC (µmol/g DW)	12.85±0.25^{d}	14.32±0.43^{c}	11.48±0.18^{e}	18.78±0.19^{a}	18.72±0.35^{a}	15.7±0.17^{b}	0.000
Total ITC (µmol/g DW)	13.21±1.47^{bc}	12.18±1.76^{bc}	9.03±0.58^{d}	14.59±0.36^{b}	24.16±2.28^{a}	10.79±0.86^{cd}	0.000
TPC (mg GAE/g DW)	1.60±0.45^{c}	2.29±0.14^{ab}	2.05±0.14^{bc}	2.21±0.14^{abc}	2.82±0.30^{a}	2.59±0.58^{ab}	0.013
TFC (mg RE/g DW)	3.13±0.253^{d}	5.47±0.38^{b}	4.42±0.37^{c}	5.69±0.31ab	6.14±0.23a	5.44±0.30^{b}	0.000
Antioxidant activity							
DPPH (mg TE/g DW)	13.67±0.54^{b}	12.71±0.37^{b}	10.45±0.55^{c}	15.51±0.83^{a}	15.61±0.46^{a}	13.01±0.38^{b}	0.000
ABTS (mg TE/g DW)	13.61±0.11^{c}	15.18±0.04^{a}	14.51±0.16^{c}	14.04±0.06^{d}	15.24±0.09^{a}	14.77±0.17^{b}	0.000

Different superscripts indicate statistical differences in the same rows (p<0.05).

Plasma treatment significantly enhanced the levels of bioactive compounds, including sinigrin, gluconapin, AITC, 3-butenyl ITC, and total ITCs, in MG microgreens compared to the control across all stages ($p < 0.05$)(Figure 2). Sinigrin levels peaked at 22.71±2.20 µmol/g DW in plasma-treated samples at 14 days, significantly higher than the control maximum of 19.52±0.24 µmol/g DW at 21 days. Similarly, gluconapin levels were markedly higher in plasma-treated samples, with a peak value of 41.81±2.10 µmol/g DW at 14 days, compared to 33.14±2.00 µmol/g DW in the control at the same stage. AITC levels in plasma-treated samples consistently surpassed control values, peaking at 8.30±0.21 µmol/g DW at 14 days. Likewise, 3-butenyl ITC levels were highest in plasma-treated samples at 18.78±0.19 µmol/g DW, significantly exceeding control values. Total ITC levels in plasma-treated samples were maximized at 24.16±2.28 µmol/g DW at 21 days, a substantial increase compared to the control. These findings highlight the efficacy of plasma treatment in enhancing the bioactive compound content in MG microgreens over various developmental stages.

For TPC and TFC, plasma treatment resulted in higher TPC, with the highest value observed at 21 days (2.82±0.30 mg GAE/g DW). A notable increase in total TFC was observed in plasma-treated microgreens, with the highest levels recorded at 21 days (6.14±0.23 mg RE/g DW), significantly higher than the control at the same time point (5.47±0.38 mg RE/g DW) ($p < 0.001$).

Likewise, for antioxidant activity, plasma treatment significantly improved the DPPH radical scavenging activity, with the highest activity at 14 days (15.51±0.83 mg TE/g DW), compared to the control (13.67±0.54 mg TE/g DW) ($p < 0.001$). ABTS radical scavenging activity was also enhanced, with plasma-treated microgreens at 21 days showing the highest activity (15.24±0.09 mg TE/g DW), significantly greater

than the control (15.18±0.04 mg TE/g DW) ($p < 0.001$). These findings suggest that plasma treatment positively impacts the bioactive compound profile and antioxidant activity of MG microgreens while altering their physical attributes over time.

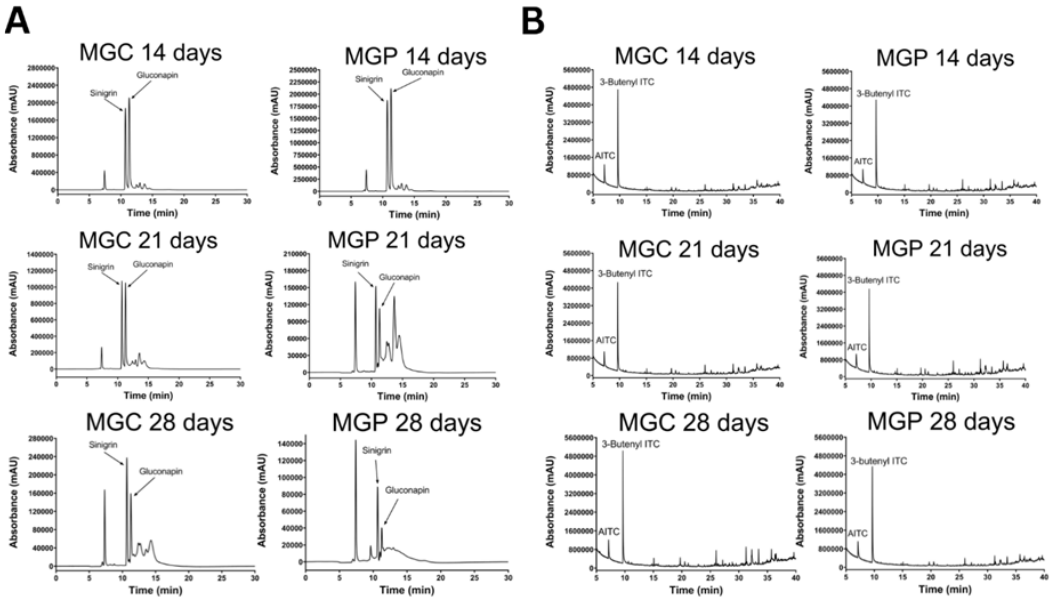

Figure 2. Chromatograms of GSLs and ITCs of MGC (Control) and MGP (Plasma) at 14,21, 28 days. (A) HPLC chromatograms of GSLs. (B) GC-MS chromatograms of ITCs.

Table 3 presents the physical and biological attributes of RTR microgreens under control and plasma-treated conditions at three different time points (14, 21, and 28 days).

Plasma treatment significantly impacted several physical and biological attributes of RTR microgreens compared to the control across different growth stages ($p < 0.05$). Stem length was notably enhanced in plasma-treated samples, peaking at 13.59±1.41 cm at 21 days, compared to the control's maximum of 12.86±1.33 cm at 14 days. Fresh and dry weights did not show significant differences between control and plasma-treated samples. Among bioactive compounds, glucoraphasatin levels were consistently higher in plasma-treated samples, reaching 16.61±0.16 μmol/g DW at 21 days, compared to 14.80±0.64 μmol/g DW in the control at 14 days. Similarly, raphasathin levels peaked in plasma-treated samples at 10.18±1.70 μmol/g DW at 21 days, significantly exceeding control levels (Figure 3A). Total ITCs were substantially increased in plasma-treated samples (Figure 3B), with a peak of 19.76±1.06 μmol/g DW at 21 days, compared to the control's maximum of 11.32±0.48 μmol/g DW at the same time point.

Plasma-treated samples also exhibited enhanced total phenolic content (TPC) and total flavonoid content (TFC), with TPC peaking at 3.99±0.21 mg GAE/g DW at 14 days and TFC at 8.54±0.43 mg RE/g DW at 21 days, significantly higher than the control. Antioxidant activities, as measured by DPPH and ABTS assays, were also significantly elevated in plasma-treated samples. DPPH activity peaked at 18.01±0.36 mg TE/g DW at 21 days, while ABTS activity was highest at 31.41±1.34 mg TE/g DW at 14 days, demonstrating the plasma treatment's ability to enhance antioxidant capacity. These findings indicate that plasma treatment effectively enhances key bioactive and antioxidant properties in RTR microgreens over growth stages (Table 3).

Table 3. Physical and biological attributes of RTR

Parameter	Rat-tailed radish (RTR)						Sig. ($p < 0.05$)
	Control 14d	Control 21d	Control 28d	Plasma 14d	Plasma 21d	Plasma 28d	
Physical							
Length of stem (cm/microgreen)	12.86±1.33^{ab}	11.94±1.34^{b}	11.89±0.75^{b}	10.48±0.81c	13.59±1.41^{a}	13.40±1.34^{a}	0.000
Fresh weight (mg/microgreen)	296.09±46.57^{a}	332.16±43.62^{a}	269.9±66.30^{a}	259.62±46.94^{a}	280.15±65.34^{a}	299.24±23.56^{a}	0.588
Dry weight (mg/microgreen)	14.94±0.34^{a}	21.71±0.60^{a}	19.81±7.44^{a}	16.15±3.04^{a}	15.21±3.49^{a}	17.37±4.16^{a}	0.293
Bioactive Compound							
Glucoraphasatin (µmol/g DW)	14.80±0.64^{b}	8.91±0.51^{c}	nd	16.25±0.17^{a}	16.61±0.16^{a}	nd	0.000
Raphasathin (µmol/g DW)	8.78±1.05^{c}	5.37±0.33^{d}	3.69±0.79^{e}	9.08±1.66^{b}	10.18±1.70^{a}	3.05±0.58^{f}	0.000
Total ITC (µmol/g DW)	10.62±0.81^{b}	11.32±0.48^{b}	10.57±2.19^{b}	12.76±1.76^{b}	19.76±1.06^{a}	12.18±1.34^{b}	0.000
TPC (mg GAE/g DW)	2.98±0.12^{b}	2.82±0.08^{bc}	2.59±0.14^{c}	3.99±0.21^{a}	3.80±0.19^{a}	2.90±0.09^{b}	0.000
TFC (mg RE/g DW)	5.37±0.20^{d}	6.33±0.21^{c}	7.22±0.35^{b}	5.82±0.32^{cd}	8.54±0.43^{a}	8.09±0.43^{a}	0.000
Antioxidant Activity							
DPPH (mg TE/g DW)	15.98±0.57^{bc}	15.66±0.46^{bc}	15.31±0.76^{c}	16.82±0.91^{b}	18.01±0.36^{a}	16.13±0.67^{bc}	0.003
ABTS (mg TE/g DW)	23.30±0.68^{b}	24.07±0.00^{b}	22.65±0.91^{b}	31.41±1.34^{a}	30.96±1.68^{a}	29.83±1.06^{a}	0.000

Different superscripts indicate statistical differences in the same rows (p<0.05). nd = not determined due to low peak area

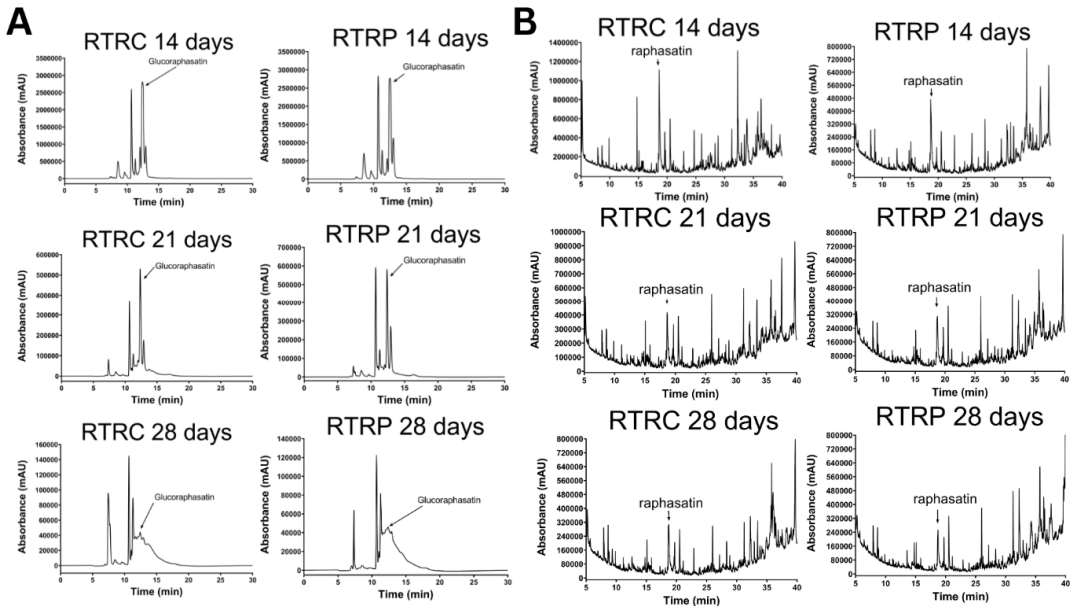

Figure 3. Chromatograms of GSLs and ITCs of RTRC (Control) and RTRP (Plasma) at 14,21, 28 days. (A) HPLC chromatograms of GSLs. (B) GC-MS chromatograms of ITCs

Nutrient and mineral content analysis

The nutrient and mineral analysis reveals distinct trends across the sample groups (Figure 4A). Copper concentrations remain consistent at < 1.0 mg/kg across all MGC, MGP, RTRC, and RTRP samples with no variation. Zinc levels are generally higher in MGP (notably peaking at 81.1 mg/kg in MGP14) compared to MGC, which exhibits lower and less variable concentrations. Similarly, RTRP samples show slightly higher zinc concentrations than RTRC, with RTRP28 exhibiting the highest zinc level of 45.3 mg/kg. Manganese

shows significant variability, with MGP28 standing out with an exceptionally high concentration of 398.1 mg/kg, while MGC samples maintain lower levels, ranging from 17.2 mg/kg to 38.9 mg/kg. Among the RTR samples, RTRC14 has the highest manganese concentration (88.8 mg/kg), while RTRP samples have generally lower levels, peaking at 44.0 mg/kg. Iron levels are substantially higher in MGP (ranging from 604.4 mg/kg to 709.0 mg/kg) compared to MGC, which ranges from 183.4 mg/kg to 318.9 mg/kg. Similarly, RTRP samples exhibit higher iron levels than RTRC, with RTRP14 showing an exceptional peak at 1240.0 mg/kg, whereas RTRC peaks at 726.0 mg/kg. These trends highlight significant elemental differences between the sample groups, particularly in manganese and iron, where MGP and RTRP show notable outliers. Plasma treatment increases nutrient and mineral concentrations overall, with notable effects on zinc, manganese, and iron, while copper remains unaffected.

Plasma treatment impacts the mineral composition variably across samples (Figure 4B). Phosphorus levels remain relatively stable, with minimal changes, though slight reductions are observed in some cases. Magnesium levels generally decrease, particularly in MGP samples, while sodium shows a significant increase in MGP21 but a reduction in RTRP28. Sulfur levels slightly increase in MGP but decrease in RTRP samples. Total nitrogen consistently increases across all plasma-treated samples, while potassium levels also show a slight overall increase, peaking in MGP28. Calcium levels decrease in MGP samples but increase slightly in RTRP samples, with RTRP28 showing the highest value among plasma-treated samples. Overall, plasma treatment tends to increase sodium, total nitrogen, potassium, and calcium (in RTRP), while reducing magnesium and calcium (in MGP) levels, with phosphorus remaining stable.

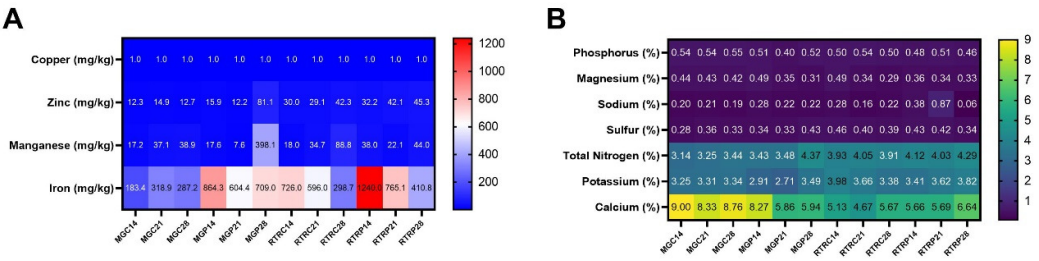

Figure 4. Heatmap of the nutrient and mineral composition across different samples. (A) Nutrient and mineral composition in mg/kg unit. (B) nutrient and mineral composition in % unit. The color intensity highlights the variation in nutrient/mineral levels, with darker colors indicating lower values and lighter colors representing higher values

Cytotoxicity

The results presented in Table 4 demonstrate the cytotoxic effects of various MG extracts on different cancer cell lines, specifically MCF-7, HeLa, HT-29, and HepG2, over three-time intervals (24 h, 48 h, and 72 h). The comparison of cytotoxicity and IC_{50} values between MGP (plasma-treated) and MGC (control) samples across cell lines (MCF-7, HeLa, HT-29, and HepG2) suggests that MGP samples are more cytotoxic overall. This is evidenced by consistently lower IC_{50} values in MGP samples compared to MGC, indicating higher potency in reducing cell viability. For example, at 72 h, MGP14 exhibits significantly lower IC_{50} values in MCF-7 (66.89 µg/mL), HeLa (21.63 µg/mL), HT-29 (78.16 µg/mL), and HepG2 (28.53 µg/mL) compared to MGC14 with IC_{50} values of 66.52 µg/mL, 16.03 µg/mL, 109.07 µg/mL, and 93.71 µg/mL, respectively. Similarly, across other time points and MGP samples, lower IC_{50} values and higher Emax values are observed, reflecting increased cytotoxic effects. The cytotoxicity trends are particularly pronounced in the HeLa and HepG2 cell lines, where plasma treatment (MGP) results in significantly reduced IC_{50} values. Therefore, MGP demonstrates enhanced cytotoxic activity, supporting its higher effectiveness compared to MGC in inhibiting cancer cell viability.

Table 4. Cytotoxicity and IC_{50} values of MG

Sample	Time (h)	*E*max (%)				IC_{50} (μg/mL)			
		MCF-7	HeLa	HT-29	HepG2	MCF-7	HeLa	HT-29	HepG2
MGC14	24 h	88.80 ± 0.35^{kA}	83.88 ± 3.19^{jB}	74.90 ± 4.38^{mC}	68.67 ± 3.21^{qD}	112.90 ± 2.34^{aC}	80.00 ± 8.75^{cD}	134.50 ± 12.27^{deB}	156.63 ± 13.52^{bA}
	48 h	91.33 ± 0.17^{fB}	95.36 ± 0.10^{cA}	84.80 ± 2.63^{iD}	88.29 ± 4.21^{eC}	77.04 ± 2.78^{kB}	16.03 ± 2.79^{oC}	119.87 ± 5.22^{efA}	119.80 ± 10.81^{cdA}
	72 h	92.57 ± 0.14^{cA}	88.07 ± 1.25^{iC}	86.59 ± 3.80^{gD}	91.33 ± 2.75^{dB}	66.52 ± 4.46^{oC}	16.03 ± 2.79^{oD}	109.07 ± 3.86^{fA}	93.71 ± 2.48^{fB}
MGC21	24 h	87.93 ± 1.50^{lA}	83.20 ± 1.59^{kB}	66.56 ± 3.33^{qD}	69.33 ± 0.33^{pC}	112.77 ± 8.57^{bC}	88.18 ± 3.30^{nD}	169.80 ± 12.97^{aA}	162.48 ± 4.86^{abB}
	48 h	90.44 ± 0.42^{hB}	95.78 ± 0.05^{bA}	83.48 ± 3.47^{lD}	84.12 ± 4.39^{jC}	90.11 ± 0.53^{fC}	87.55 ± 4.40^{nD}	$121.00\pm4.16c^{fB}$	129.73 ± 3.88^{cA}
	72 h	92.48 ± 0.36^{cB}	94.90 ± 0.10^{cA}	86.31 ± 3.80^{hD}	88.06 ± 3.31^{fC}	65.85 ± 2.75^{pC}	62.45 ± 2.88^{qD}	119.10 ± 9.28^{fA}	104.69 ± 4.89^{efB}
MGC28	24 h	90.18 ± 0.18^{iA}	83.56 ± 2.89^{jB}	71.55 ± 3.73^{nC}	67.02 ± 0.55^{rD}	90.27 ± 2.73^{eC}	75.65 ± 3.89^{qD}	158.47 ± 11.46^{abB}	171.50 ± 4.78^{aA}
	48 h	92.41 ± 0.09^{cdB}	95.36 ± 0.13^{cA}	89.28 ± 3.82^{eC}	79.19 ± 6.32^{mD}	78.21 ± 1.00^{jD}	79.40 ± 2.78^{eC}	114.80 ± 10.41^{fA}	111.61 ± 11.35^{deB}
	72 h	92.30 ± 0.08^{dC}	94.91 ± 0.12^{cA}	92.77 ± 4.44^{aB}	91.01 ± 2.01^{dD}	72.37 ± 3.17^{mC}	42.75 ± 8.45^{jD}	86.02 ± 5.60^{ghA}	79.77 ± 0.10^{gB}
MGP14	24 h	88.53 ± 1.03^{kA}	82.31 ± 2.26^{lB}	71.22 ± 4.74^{oD}	80.77 ± 0.77^{fC}	98.65 ± 4.17^{dB}	45.1 ± 2.16^{tD}	140.03 ± 6.04^{cdA}	61.14 ± 0.37^{hC}
	48 h	91.86 ± 0.80^{eB}	96.33 ± 0.11^{aA}	83.82 ± 2.44^{kD}	87.35 ± 0.97^{fC}	76.37 ± 6.21^{lB}	30.86 ± 2.97^{muD}	93.99 ± 11.14^{gA}	38.41 ± 1.67^{iC}
	72 h	91.28 ± 0.82^{fC}	94.90 ± 0.21^{cA}	87.04 ± 2.05^{fD}	92.59 ± 0.79^{bB}	66.89 ± 6.00^{nB}	21.63 ± 1.92^{nuD}	78.16 ± 7.11^{hA}	28.53 ± 2.16^{iC}
MGP21	24 h	90.89 ± 0.67^{gB}	94.39 ± 1.36^{fA}	70.82 ± 1.72^{pD}	78.28 ± 5.06^{oC}	88.71 ± 5.80^{gC}	72.52 ± 3.86^{eD}	112.03 ± 10.73^{fB}	128.70 ± 13.23^{cA}
	48 h	94.47 ± 0.32^{aB}	94.73 ± 0.09^{cA}	88.07 ± 7.12^{eC}	86.29 ± 1.74^{iD}	83.86 ± 3.58^{iC}	61.13 ± 5.65^{qD}	110.43 ± 5.76^{fA}	97.21 ± 6.39^{fB}
	72 h	89.89 ± 1.95^{jD}	93.05 ± 0.08^{hA}	92.19 ± 5.06^{bC}	92.89 ± 0.59^{aB}	56.91 ± 6.10^{qC}	34.40 ± 0.44^{kD}	93.93 ± 5.91^{gA}	72.57 ± 2.91^{ghB}
MGP28	24 h	94.25 ± 0.37^{bA}	94.25 ± 0.52^{fA}	66.16 ± 4.21^{rC}	74.29 ± 5.67^{nB}	101.74 ± 3.03^{cD}	85.85 ± 1.32^{bE}	150.73 ± 10.70^{bcA}	129.23 ± 13.7^{cC}
	48 h	90.20 ± 1.40^{iB}	95.12 ± 0.14^{dA}	84.47 ± 6.81^{jC}	83.68 ± 2.18^{kD}	87.70 ± 3.68^{hC}	59.05 ± 0.80^{hD}	93.62 ± 5.31^{gB}	101.97 ± 7.23^{efA}
	72 h	89.89 ± 1.96^{jB}	94.00 ± 0.13^{gA}	88.85 ± 2.28^{dB}	87.12 ± 4.84^{hC}	56.92 ± 6.10^{qC}	32.08 ± 3.69^{jD}	86.37 ± 2.55^{ghA}	80.04 ± 5.00^{gB}

Different small letters in columns indicate statistical differences ($p \leq 0.05$). Capital letters in the rows indicate statistical differences ($p \leq 0.05$).

The comparison of cytotoxicity and IC_{50} values between RTRP (plasma-treated) and RTRC (control) samples across cell lines (MCF-7, HeLa, HT-29, and HepG2) suggests that RTRP samples are more cytotoxic overall (Table 5). This is evident from consistently lower IC_{50} values in RTRP samples compared to RTRC, indicating higher potency in reducing cell viability. For instance, at 72 h, RTRP21 exhibits significantly lower IC_{50} values in MCF-7 (20.72 μg/mL), HeLa (30.87 μg/mL), HT-29 (52.64 μg/mL), and HepG2 (63.56 μg/mL) compared to RTRC21 with IC_{50} values of 50.77 μg/mL, 11.82 μg/mL, 72.03 μg/mL, and 95.18 μg/mL, respectively. Similar trends are observed in other RTRP samples, where plasma treatment significantly reduces IC_{50} values across most cell lines. Additionally, RTRP samples exhibit higher Emax values in most cases, reflecting increased cytotoxic activity. The enhanced cytotoxicity is especially notable in MCF-7 and HT-29 cell lines, where RTRP samples consistently outperform RTRC controls. Overall, these results highlight the greater cytotoxic potential of plasma-treated RTRP samples compared to RTRC controls.

Table 5. Cytotoxicity and IC_{50} values of RTR

Sample	Time (h)	*E*max (%)				IC_{50} (µg/ml)			
		MCF-7	HeLa	HT-29	HepG2	MCF-7	HeLa	HT-29	HepG2
RTRC14	24 h	89.87±0.76^{iB}	94.28±0.24^{abcA}	83.03±3.41^{nC}	66.52±3.76^{tD}	74.39±6.52^{gC}	26.52±1.29^{iD}	88.89±7.45^{cB}	121.50±1.71^{bA}
	48 h	92.86±0.00^{dB}	95.24±0.23^{abA}	85.43±0.62^{kD}	90.33±0.76^{cC}	46.14±2.87^{mC}	19.10±2.77^{kD}	77.65±4.91^{deA}	54.48±2.24^{ghB}
	72 h	93.19±0.08^{cA}	91.87±0.78^{cdB}	89.29±3.97^{fC}	88.75±0.36^{fD}	42.00±2.93^{nC}	18.25±1.19^{lD}	74.30±6.56^{defA}	49.70±0.89^{hiB}
RTRC21	24 h	89.33±0.22^{jB}	94.13±0.40^{abcA}	75.98±3.62^{oC}	73.72±2.94^{sD}	75.00±5.57^{fC}	42.40±1.18^{fD}	109.04±11.32^{bB}	138.87±13.52^{aA}
	48 h	92.03±0.27^{hiB}	95.83±0.08^{aA}	90.67±2.32^{eC}	76.75±1.67^{fD}	64.64±2.30^{iC}	25.25±3.42^{jD}	79.46±4.39^{cdeB}	112.63±12.99^{bA}
	72 h	92.79±0.09^{dA}	88.04±0.38^{gB}	88.20±1.18^{gB}	84.58±1.35^{jC}	50.77±6.69^{mC}	11.82±1.37^{nD}	72.03±3.37^{efgB}	95.18±2.82^{cA}
RTRC28	24 h	89.00±0.20^{kB}	94.36±0.33^{abcA}	72.93±5.77^{pC}	70.00±4.48^{pD}	97.44±5.31^{eC}	59.22±1.79^{eD}	113.83±6.64^{bB}	150.10±12.39^{aA}
	48 h	92.05±0.09^{hiB}	95.67±0.17^{aA}	86.09±2.79^{iC}	85.09±1.32^{iD}	72.55±2.27^{hiB}	11.87±0.96^{nD}	67.02±2.04^{fghC}	91.77±7.03^{cdA}
	72 h	92.64±0.14^{deiB}	88.70±1.27^{fC}	83.97±1.44^{mD}	93.54±0.75^{aA}	61.64±5.22^{jC}	11.85±0.40^{nD}	63.34±2.85^{ghiB}	65.89±5.08^{efgA}
RTRP14	24 h	93.93±0.63^{hiB}	94.87±0.15^{abcA}	91.70±0.38^{dC}	75.75±1.74^{mD}	95.35±2.17^{cB}	51.83±1.16^{eC}	45.42±0.60^{ikD}	98.32±11.58^{cA}
	48 h	89.13±0.22^{jkC}	95.36±0.05^{abA}	94.21±0.76^{bB}	80.45±2.96^{kD}	51.01±2.42^{lB}	14.44±0.96^{nD}	43.59±1.44^{ijkC}	72.63±6.26^{efA}
	72 h	92.53±0.81^{efA}	89.36±0.50^{eC}	83.97±1.44^{mD}	91.50±0.73^{cB}	27.98±1.16^{qC}	13.35±0.46^{oD}	37.34±3.36^{klB}	64.59±1.50^{efghA}
RTRP21	24 h	93.97±0.60^{bB}	94.51±0.47^{abcA}	86.70±3.56^{hC}	73.57±1.64^{oD}	95.32±2.25^{dC}	86.39±2.73^{aD}	103.96±9.63^{bB}	139.13±9.92^{aA}
	48 h	92.19±0.41^{fgC}	95.36±0.00^{abA}	94.88±2.04^{aB}	85.53±2.06^{hD}	29.85±1.36^{pD}	56.17±6.94^{dC}	60.36±1.22^{hiB}	79.17±9.69^{deA}
	72 h	94.57±0.14^{aA}	90.90±0.85^{dD}	93.29±0.25^{cB}	92.33±0.09^{bC}	20.72±0.69^{rD}	30.87±2.49^{kC}	52.64±0.48^{ijB}	63.56±1.66^{fghA}
RTRP28	24 h	88.67±0.42^{lB}	94.47±0.10^{abcA}	69.54±3.18^{qC}	68.56±3.98^{qD}	97.42±9.40^{bC}	74.93±4.20^{bD}	151.43±11.32^{aA}	150.9311.13^{aB}
	48 h	90.10±1.57^{iB}	95.42±0.00^{abA}	85.37±1.48^{lD}	87.39±4.87^{gC}	81.08±7.86^{eC}	15.91±1.98^{mD}	84.56±0.46^{cdB}	88.23±8.74^{cdA}
	72 h	89.89±1.96^{jC}	94.00±0.13^{abcA}	86.59±5.34^{iD}	91.11±2.43^{dB}	56.92±6.10^{kC}	32.08±3.69^{gD}	81.94±3.32^{cdeA}	59.54±5.11 ^{fghB}

Different small letters in columns indicate statistical differences ($p \leq 0.05$). Capital letters in the rows indicate statistical differences ($p \leq 0.05$).

Cell morpholocial changes and DNA fragmentation

Since the bioactive compounds, bioactivities, and anticancer properties of MG and RTR are most prominent at 21 days, plants from both the control and plasma-treated groups at this age were selected for further detailed analysis.

The comparison of cell morphological changes between MGC vs. MGP and RTRC vs. RTRP reveals that plasma treatment significantly enhances cytotoxic effects (Figure 5). In HepG2 cells, MGC and RTRC treatments result in moderate cell death, with some intact cells visible. However, MGP and RTRP treatments cause more pronounced structural damage and widespread cell death, as indicated by fragmented and shrunken cells. In MCF-7 cells, MGC and RTRC induce partial cell death, with visible debris and some intact cells. Plasma-treated samples (MGP and RTRP) exhibit significantly greater cytotoxicity, with extensive cellular disintegration and detachment. Similarly, in HeLa cells, MGC and RTRC treatments lead to rounded and shrunken cells, while MGP and RTRP cause severe structural loss and cell debris, indicating enhanced effectiveness of plasma treatment. For HT-29 cells, MGC and RTRC treatments cause some cell death with observable detached cells. MGP and RTRP treatments result in extensive morphological damage, characterized by a complete loss of structural integrity and increased cell debris. Overall, plasma-treated samples (MGP and RTRP) consistently exhibit higher cytotoxicity compared to controls (MGC and RTRC) across all cell lines. The enhanced cell death and severe morphological changes, such as detachment, fragmentation, and loss of cellular integrity, confirm the superior potency of plasma-treated samples in inducing cytotoxic effects. This suggests that plasma treatment significantly amplifies the ability of MG and RTR to target and destroy cancer cells.

DNA fragmentation analysis demonstrates that plasma-treated samples (MGP and RTRP) induce significantly higher levels of apoptosis compared to controls (MGC and RTRC) across HepG2, MCF-7, HeLa, and HT-29 cell lines (Figure 6). Untreated cells show intact DNA, while MGC and RTRC treatments cause moderate DNA fragmentation. In contrast, MGP and RTRP treatments result in pronounced DNA laddering, a hallmark of apoptosis, particularly in MCF-7 and HeLa cells. The enhanced DNA damage in plasma-treated samples confirms their stronger cytotoxic and pro-apoptotic effects, indicating that plasma treatment significantly amplifies the apoptotic potential of MG and RTR in cancer cells.

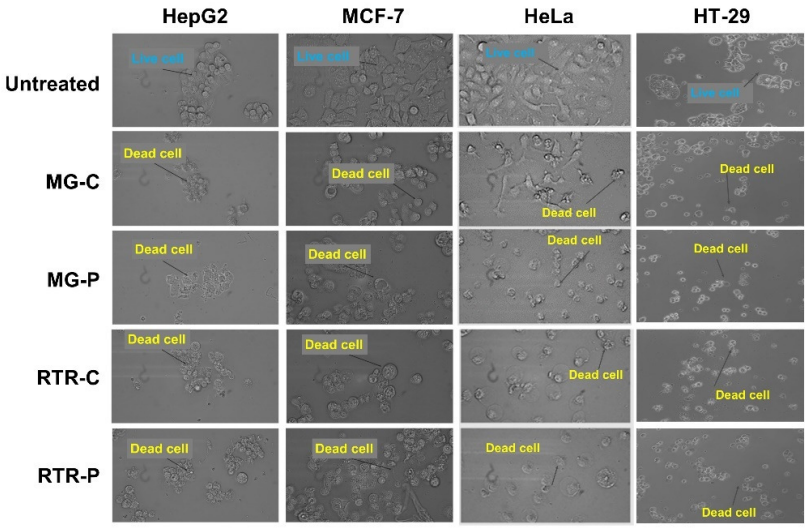

Figure 5. Cell morphological changes of HepG2, MCF-7, HeLa and HT-29 upon MG and RTR

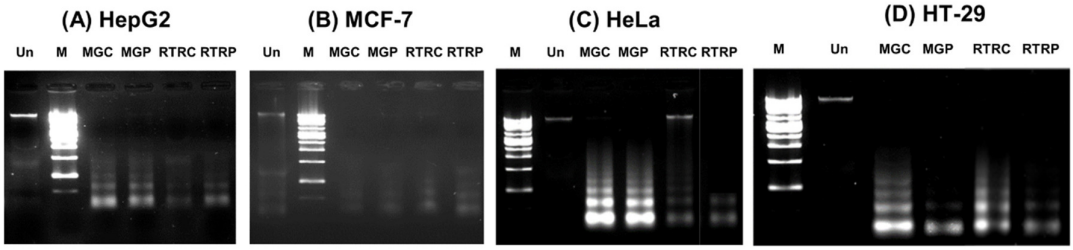

Figure 6. DNA fragmentation of HepG2, MCF-7, HeLa and HT-29 upon MG and RTR treatment

Figure 7 illustrates the anti-migratory activity of MG and RTR on MCF-7, HeLa, HepG2, and HT-29 cells over 48 h (Figure 7).

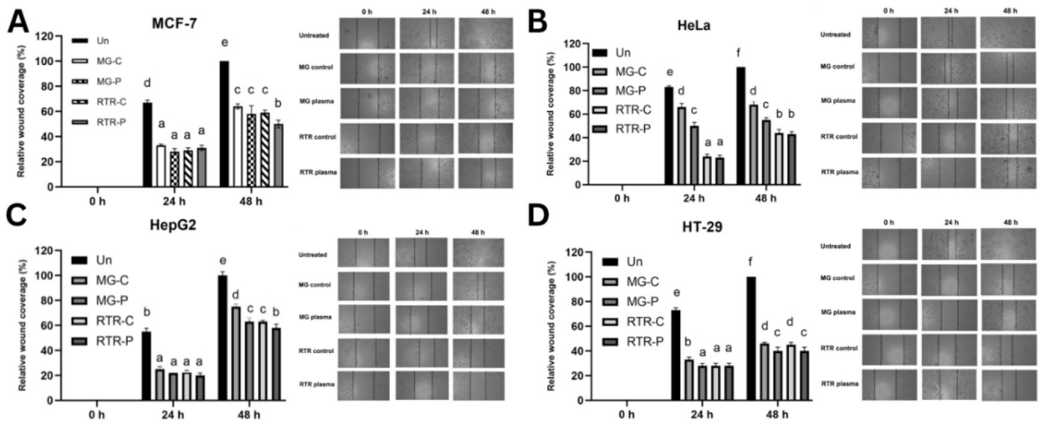

Figure 7. Anti-migratory activity of MG and RTR treatment on HepG2, MCF-7, HeLa and HT-29

Wound healing assays were performed to assess cell migration, represented as the relative wound coverage (%) at 0 h, 24 h, and 48 h post-treatment. For all four cell lines, the untreated (Un) groups demonstrated robust wound closure within 48 h, showing minimal inhibition of migration. In contrast, both control (MG-C and RTR-C) and plasma-treated (MG-P and RTR-P) microgreen groups exhibited significant

reductions in wound closure compared to untreated groups. Plasma-treated microgreens (MG-P and RTR-P) consistently showed the strongest anti-migratory effects across all cell lines (Figure 7).

Gene and protein expressions

Figure 8-11 show the relative mRNA expression levels of key apoptotic genes (such as *cytochrome c*, *caspase-3*, and *p21*) in MCF-7, HeLa, HT-29 and HepG2 cells after treatment with MG microgreens (MG-C and MG-P) and RTR microgreens (RTR-C and RTR-P). The untreated (Un) groups served as a baseline for comparison. In all four cancer cells, *cytochrome c* mRNA expression was significantly upregulated in upon treatment with plasma-treated microgreens (MG-P and RTR-P) compared to untreated and control groups (MG-C and RTR-C). *Caspase-3* expression, another key player in the apoptosis pathway, followed a similar trend, with a marked increase in expression in MG-P and RTR-P treatments in comparison to untreated and control groups. The gene *p21* expression, a well-known cell cycle regulator involved in apoptosis, was notably elevated in the plasma-treated microgreen groups, particularly in MCF-7 and HeLa cells. The upregulation of these genes indicates that plasma-treated microgreens likely activate intrinsic apoptotic pathways across these cancer cell lines, as evidenced by the increased transcription of key apoptotic regulators.

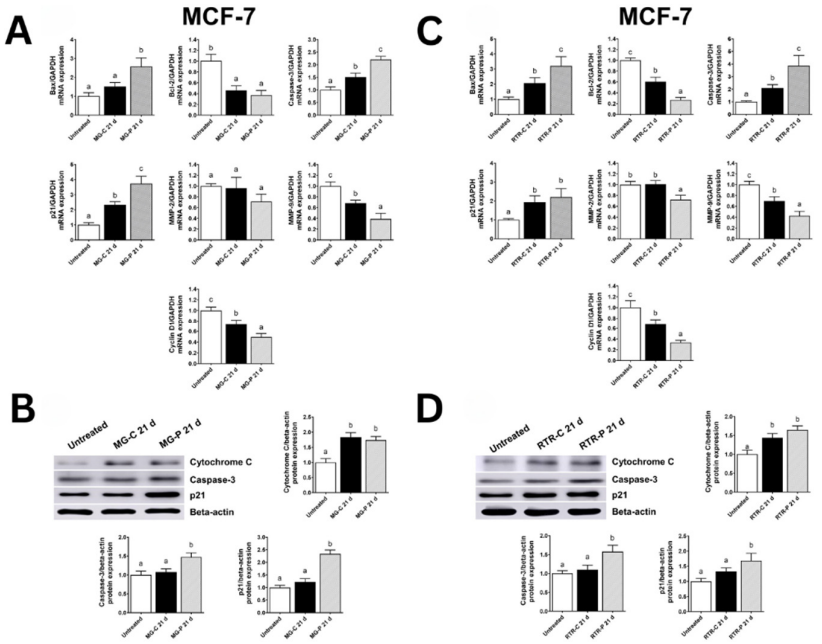

Figure 8. Gene and protein expressions of MCF-7 upon MG and RTR treatment. (A) Gene expressions in MG. (B) Protein expressions in MG. (C) Gene expression in RTR. (D) Protein expression in RTR

Figures 8-11 also display the corresponding protein expression levels of cytochrome c, caspase-3, and p21 in HepG2, MCF-7, HeLa, and HT-29 cells after treatment with MG-C, MG-P, RTR-C, and RTR-P microgreens. Western blot analysis was used to quantify protein expression, with beta-actin serving as the loading control. Cytochrome c protein levels were significantly higher in plasma-treated groups (MG-P and RTR-P) compared to untreated and control groups, corroborating the mRNA expression data. This elevation suggests that the plasma-treated microgreens effectively induce mitochondrial release of cytochrome c, a key step in apoptosis initiation. Caspase-3 protein activation was also elevated in MG-P and RTR-P treatments, confirming the activation of the caspase cascade, which is critical for the execution phase of apoptosis. The p21 protein levels were similarly upregulated in plasma-treated microgreen groups, particularly in HeLa and MCF-7 cells, suggesting that these treatments not only induce apoptosis but may also cause cell cycle arrest. The

protein expression data align with the gene expression results, indicating that plasma-treated microgreens modulate both transcriptional and translational levels of apoptotic pathways in HepG2, MCF-7, HeLa, and HT-29 cells.

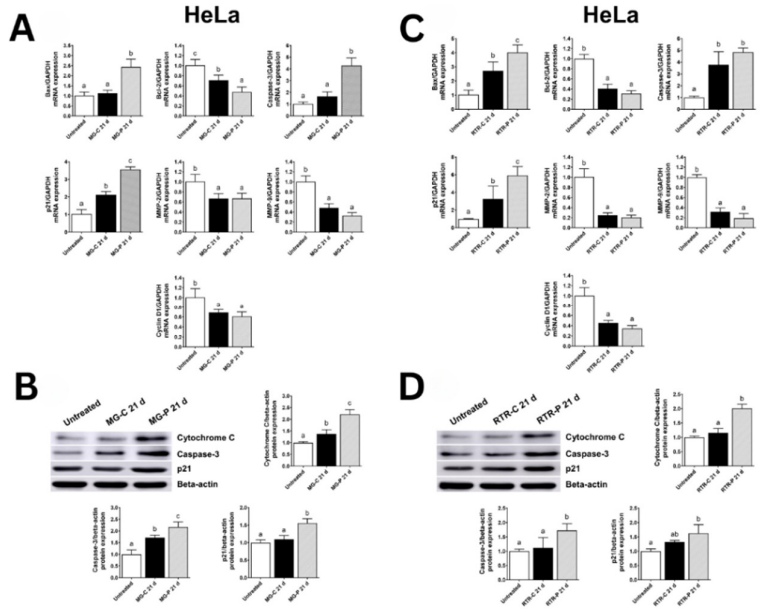

Figure 9. Gene and protein expressions of HeLa upon MG and RTR treatment. (A) Gene expressions in MG. (B) Protein expressions in MG. (C) Gene expression in RTR. (D) Protein expression in RTR

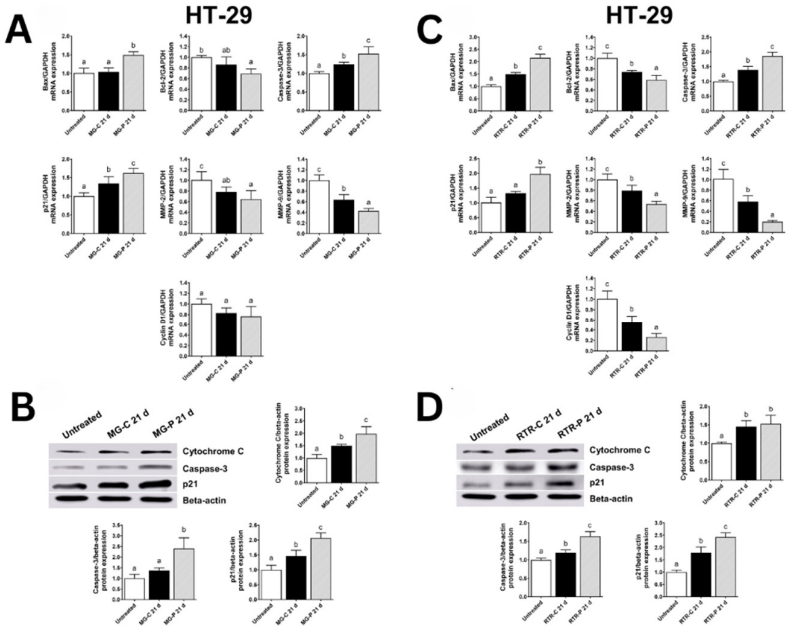

Figure 10. Gene and protein expressions of HT-29 upon MG and RTR treatment. (A) Gene expressions in MG. (B) Protein expressions in MG. (C) Gene expression in RTR. (D) Protein expression in RTR

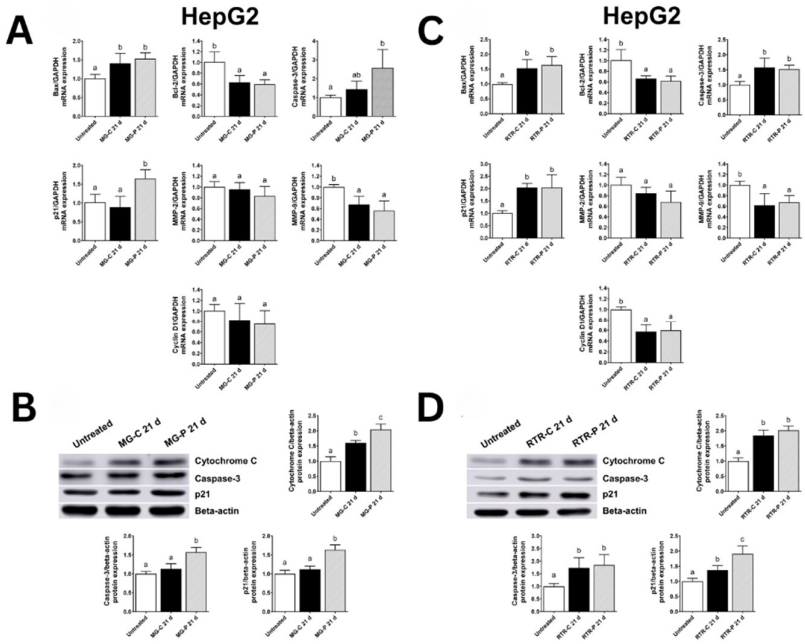

Figure 11. Gene and protein expressions of HepG2 upon MG and RTR treatment. (A) Gene expressions in MG. (B) Protein expressions in MG. (C) Gene expression in RTR. (D) Protein expression in RTR

Discussion

The current study demonstrates the multifaceted impact of non-thermal plasma (NTP) seed priming and early developmental stages on two Thai cruciferous plants, MG and RTR, with notable improvements in GSL and ITC contents, antioxidant and anticancer activities, and changes in physical and biological attributes. The findings indicate that NTP treatment not only modifies seed morphology but also influences plant growth and the accumulation of bioactive compounds, which are crucial for both nutritional and therapeutic applications.

Air NTP enhances seed performance by generating reactive oxygen and nitrogen species (ROS and RNS), such as O_3, OH•, NO, and N_2^*, which modify the seed surface and internal biochemistry. In our study, Optical Emission Spectroscopy (OES) confirmed the presence of key radical species in Air NTP (data are not shown here), which play a crucial role in enhancing seed germination and growth. These findings align with the previous observations (Matra, 2018; Tanakaran and Matra, 2022), demonstrating that plasma-generated ROS and RNS contribute to beneficial biochemical modifications during seed treatment.

For seed morphological changes and growth performance, it was revealed that notable morphological changes in the seed coats of both MG and RTR following NTP treatment occurred. Control seeds exhibited a rough and porous surface, while plasma-treated seeds displayed a smoother surface with reduced porosity, suggesting enhanced water absorption capabilities. This morphological alteration is significant as it may facilitate improved germination and early growth, aligning with previous studies that indicate that seed priming can enhance metabolic processes and improve germination rates (Kanjevac *et al*., 2022). Plasma treatment enhances surface smoothing and improves the wettability of the seed surfaces in two Brassicaceae species, *Arabidopsis thaliana* and *Camelina sativa* (Bafoil *et al.,* 2021*)*.

In terms of plant growth, the results demonstrated that while plasma treatment suppressed the growth of MG microgreens, it significantly enhanced the growth of RTR microgreens, particularly at 21- and 28-days post-treatment. The differential growth responses of MG and RTR to NTP treatment can be attributed to their unique metabolic pathways and resource allocation strategies. For MG, the suppression of growth,

particularly in terms of stem length and overall biomass, suggests a potential redirection of energy towards the synthesis of secondary metabolites, such as GSLs and ITCs. This phenomenon aligns with existing literature that posits that stress conditions, including those induced by plasma treatment, can stimulate the production of secondary metabolites as a defensive mechanism against biotic and abiotic stresses (Kanjevac *et al*., 2022). The elevated levels of GSLs and ITCs in plasma-treated MG microgreens indicate that the plant may prioritize chemical defenses over growth, a strategy that could enhance its survival and competitive advantage in natural ecosystems (Baenas *et al*., 2012).

Moreover, the bioactive compound profiles were markedly enhanced in plasma-treated microgreens. Notably, levels of GSLs, as well as ITCs, were significantly higher in plasma-treated plants compared to controls. The observed increases in bioactive compounds following NTP treatment may be attributed to the activation of specific signaling pathways that upregulate the expression of genes involved in GSL biosynthesis and thus ITCs, thereby contributing to the plants' defensive mechanisms against potential threats (Lyu *et al*., 2023). In addition, the peak levels of bioactive compounds observed at specific growth stages emphasize the critical role of timing in harvesting microgreens for optimal nutritional and functional benefits. The findings from this study are consistent with the work of Pérez-Balibrea *et al*. (2011), who demonstrated that the developmental stage of plants significantly influences GSL content. Harvesting microgreens at the right time can maximize their health-promoting properties, making it essential for growers to consider the timing of NTP treatment and subsequent harvesting to enhance the nutritional value of their crops. The increased TPC and TFC further indicate that NTP treatment can enhance the nutritional quality of these microgreens, which is consistent with previous research suggesting that environmental stressors can elevate phytochemical levels in plants (Lyu *et al*., 2023).

Likewise, plasma treatment significantly enhanced antioxidant activity in both MG and RTR microgreens, as measured by DPPH and ABTS assays. These improvements are attributable to elevated phenolic and flavonoid contents, which are well-documented antioxidants (Hussain *et al*., 2018). The highest antioxidant activities were observed at 14 and 21 days for MG and RTR, respectively, corresponding to the peaks in TPC and TFC. Such correlations suggest a direct link between phenolic compounds and the enhanced antioxidant potential of plasma-treated microgreens. These findings align with those of Sarangapani *et al*. (2017), who demonstrated that plasma treatment enhances phenolic biosynthesis by activating phenylpropanoid pathways. The increased antioxidant activity not only enhances the nutritional value of MG and RTR but also suggests their potential use in functional foods or nutraceuticals.

In addition, plasma treatment significantly increased trace elements like zinc, manganese, and iron in MG and RTR microgreens. These minerals play crucial roles in human health, particularly in enzymatic functions and antioxidant defense systems (Motrescu *et al*., 2023). Previously, in *Begonia cucullata* Willd., NTP treatment influenced mineral content, increasing zinc and silicon concentrations in white flowers while reducing potassium, magnesium, and manganese levels (Traversari *et al*., 2021). Such alterations enhance the nutritional value of microgreens, making them more suitable for functional food applications.

Furthermore, plasma-treated MG and RTR microgreens exhibited significantly enhanced cytotoxic effects against four cancer cell lines (MCF-7, HeLa, HT-29, and HepG2), as evidenced by lower IC50 values and increased *E*max percentages. The increased cytotoxicity is likely linked to the elevated ITC levels, particularly AITC and 3-butenyl ITC, which are known to induce apoptosis in cancer cells via reactive oxygen species (ROS) generation and mitochondrial dysfunction (Rajakumar and Pugalendhi, 2024; Arora *et al*., 2016). Morphological changes and DNA fragmentation analyses further corroborated the apoptotic effects of plasma-treated samples, highlighting the activation of intrinsic apoptosis pathways. Upregulated expression of apoptotic genes (e.g., *cytochrome c*, *caspase-3*, *p21*) and their corresponding proteins supports the mechanistic role of plasma treatment in enhancing anticancer properties (Wang *et al*., 2024). Notably, plasma-treated MG exhibited stronger cytotoxic effects on HeLa and HepG2 cells, while RTR showed higher potency against MCF-7 and HT-29 cells. Such specificity may result from differential bioactive compound profiles and their

varying efficacy against distinct cancer types. The strong anti-migratory effects of plasma-treated MG and RTR against cancer cell lines, demonstrated by wound healing assays, highlight their potential in inhibiting metastasis. This effect is likely mediated by ITCs, which have been shown to downregulate epithelial-mesenchymal transition (EMT) markers and inhibit cancer cell migration (Saengha *et al*., 2021). The enhanced anti-migratory activity observed in plasma-treated samples further underscores the therapeutic potential of these microgreens.

Future research should explore the underlying molecular mechanisms driving these enhancements, particularly the signaling pathways activated by plasma treatment. Additionally, in *vivo* studies are essential to validate the anticancer efficacy of plasma-treated microgreens and assess their safety profiles. The scalability of plasma treatment technology and its economic feasibility for large-scale agricultural applications should also be investigated.

Conclusions

This study highlights the positive impact of plasma treatment on MG and RTR microgreens, focusing on seed morphology, growth, bioactive compounds, and anticancer properties. Plasma treatment altered seed coat morphology, enhancing water absorption, accelerating germination, and promoting more vigorous growth compared to untreated seeds. Plasma-treated microgreens exhibited longer stems, increased fresh and dry weight, and higher concentrations of bioactive compounds, including ITCs, TPC and TFC, which boosted their antioxidant activity. Cytotoxicity assays on four cancer cell lines (MCF-7, HeLa, HT-29, and HepG2) showed that plasma-treated MG and RTR microgreens induced significant apoptosis, as evidenced by cell morphology changes, DNA fragmentation, and the upregulation of apoptotic genes (*cytochrome c*, *caspase-3*, and *p21*) and corresponding proteins. These effects were stronger in plasma-treated microgreens, which also demonstrated anti-migratory activity in wound healing assays, indicating their potential as natural anticancer agents. In conclusion, plasma treatment enhances both the growth performance and bioactive properties of MG and RTR microgreens, making them promising functional foods with potential health benefits, particularly in cancer prevention and treatment.

Authors' Contributions

The authors are responsible for any claims arising from the content of this article and will be held liable for any damages. Testing was carried out by T.K., W.S., K.N., K.M., P.P., P.K., and T.B. The tests were devised by B.B. and S.D. T.K. collected and sorted the cancer cells. V.L. received the funding, conducted the experiments, evaluated the data, wrote and revised the manuscript. All authors read and approved the final manuscript.

Ethical approval (for researches involving animals or humans)

Not applicable.

Acknowledgements

This research project was financially supported by Mahasarakham University.

Conflict of Interests

The authors declare that there are no conflicts of interest related to this article.

References

Arora R, Kumar R, Mahajan J, Vig AP, Singh B, Singh B, Arora S (2016). 3-Butenyl isothiocyanate: A hydrolytic product of glucosinolate as a potential cytotoxic agent against human cancer cell lines. Journal of Food Science and Technology 53:3437-3445. *https://doi.org/10.1007/s13197-016-2316-7*

Baenas N, Moreno DA, García-Viguera C (2012). Selecting sprouts of brassicaceae for optimum phytochemical composition. Journal of Agricultural and Food Chemistry 60(45):11409-11420. *https://doi.org/10.1021/jf302863c*

Bafoil M, Yousfi M, Dunand C, Merbahi N (2021). Effects of dielectric barrier ambient air plasma on two Brassicaceae seeds: *Arabidopsis thaliana* and *Camelina sativa*. International Journal of Molecular Sciences 22(18):9923. *https://doi.org/10.3390/ijms22189923*

Bhabani MG, Shams R, Dash KK (2024). Microgreens and novel non-thermal seed germination techniques for sustainable food systems: A review. Food Science and Biotechnology 33(7):1541-1557. *https://doi.org/10.1007/s10068-024-01529-9*

Blažević I, Montaut S, Burčul F, Olsen CE, Burow M, Rollin P, Agerbirk N (2020). Glucosinolate structural diversity, identification, chemical synthesis, and metabolism in plants. Phytochemistry 169:112100. *https://doi.org/10.1016/j.phytochem.2019.112100*

Ferlay J, Ervik M, Lam F, Laversanne M, Colombet M, Mery L, Piñeros M, Znaor A, Soerjomataram I, Bray F (2024). Global Cancer Observatory: Cancer Today. Lyon, France: International Agency for Research on Cancer. *https://gco.iarc.who.int/today*

Fujioka N, Fritz V, Upadhyaya P, Kassie F, Hecht S (2016). Research on cruciferous vegetables, indole-3-carbinol, and cancer prevention: A tribute to Lee W. Wattenberg. Molecular Nutrition and Food Research 60(6):1228-1238. *https://doi.org/10.1002/mnfr.201500889*

Hussain S, Fareed S, Ansari S, Rahman MA, Ahmad IZ, Saeed M (2018). Current approaches toward production of secondary plant metabolites. Journal of Pharmacy and Bioallied Sciences 4(1):10-20. *https://doi.org/10.4103/0975-7406.92725*

Jia H, Jia Y, Ren F, Liu H (2024). Enhancing bioactive compounds in plant-based foods: Influencing factors and technological advances. Food Chemistry 460(Pt 3):140744. *https://doi.org/10.1016/j.foodchem.2024.140744*

Kanjevac M, Jakovljević D, Todorović M, Stanković M, Ćurčić S, Bojović B (2022). Improvement of germination and early growth of radish (*Raphanus sativus* L.) through modulation of seed metabolic processes. Plants 11(6):757. *https://doi.org/10.3390/plants11060757*

Karirat T, Deeseenthum S, Ma NL, Sutthi N, Luang-In V (2024). Utilisation of agricultural residues for antioxidant exopolysaccharide production by Bacillus *spp*. Natural Product Research 38(7):1-4. *https://doi.org/10.1080/14786419.2024.2398720*

Li YZ, Yang ZY, Gong TT, Liu YS, Liu FH, Wen ZY, ... Wu QJ (2022). Cruciferous vegetable consumption and multiple health outcomes: An umbrella review of 41 systematic reviews and meta-analyses of 303 observational studies. Food & Function 13(8):4247-4259. *https://doi.org/10.1039/d1fo03094a*

Luang-In V, Narbad A, Nueno-Palop C, Mithen R, Bennett M, Rossiter JT (2014). The metabolism of methylsulfinylalkyl- and methylthioalkyl-glucosinolates by a selection of human gut bacteria. Molecular Nutrition and Food Research 58:875-883. *https://doi.org/10.1002/mnfr.201300377*

Luang-In V, Deeseenthum S, Udomwong P, Saengha W, Gregori M (2018). Formation of sulforaphane and iberin products from Thai cabbage fermented by myrosinase-positive bacteria. Molecules 23(4):955. *https://doi.org/10.3390/molecules23040955*

Luang-In V, Saengha W, Karirat T, Buranrat B, Matra K, Deeseenthum S, Katisart T (2021). Effect of cold plasma and elicitors on bioactive contents, antioxidant activity and cytotoxicity of Thai rat-tailed radish microgreens. Journal of the Science of Food and Agriculture 101(4):1685-1698. *https://doi.org/10.1002/jsfa.10985*

Lyu X, Chen Y, Gao S, Cao W, Fan D, Duan Z, Xia Z (2023). Metabolomic and transcriptomic analysis of cold plasma promoting biosynthesis of active substances in broccoli sprouts. Phytochemical Analysis 34(8):925-937. *https://doi.org/10.1002/pca.3256*

Matra K (2018). Atmospheric non-thermal argon-oxygen plasma for sunflower seedling growth improvement. Japanese Journal of Applied Physics 57(1):01AG03. *https://doi.org/10.7567/JJAP.57.01AG03*

Mir SA, Shah MA, Mir MM (2017). Microgreens: Production, shelf life, and bioactive components. Critical Reviews in Food Science and Nutrition 57(12):2730-2736. *https://doi.org/10.1080/10408398.2016.1144557*

Morrison M, Joseph J, McCann S, Tang L, Almohanna H, Moysich K (2019). Cruciferous vegetable consumption and stomach cancer: A case-control study. Nutrition and Cancer 72(1):52-61. *https://doi.org/10.1080/01635581.2019.1615100*

Motrescu I, Ciolan MA, Calistru AE, Jitareanu G (2023). Germination and growth improvement of some microgreens under the influence of reactive species produced in a non-thermal plasma (NTP). Agronomy 13(1):150. *https://doi.org/10.3390/agronomy13010150*

Nandini DB, Rao RS, Deepak BS, Reddy PB (2020). Sulforaphane in broccoli: The green chemoprevention!! Role in cancer prevention and therapy. Journal of Oral and Maxillofacial Pathology 24(2):405. *https://doi.org/10.4103/jomfp.JOMFP_126_19*

Pérez-Balibrea S, Moreno DA, García-Viguera C (2011). Improving the phytochemical composition of broccoli sprouts by elicitation. Food Chemistry 129(1):35-44. *https://doi.org/10.1016/j.foodchem.2011.04.066*

Rajakumar T, Pugalendhi P (2024). Allyl isothiocyanate regulates oxidative stress, inflammation, cell proliferation, cell cycle arrest, apoptosis, angiogenesis, invasion, and metastasis via interaction with multiple cell signaling pathways. Histochemistry and Cell Biology 161:211-221. *https://doi.org/10.1007/s00418-023-02255-9*

Saengha W, Karirat T, Pitisin N, Plangklang S, Butkhup L, Udomwong P, ... Luang-In V (2024). Exploring the bioactive potential of *Calostoma insigne*, an endangered culinary puffball mushroom, from Northeastern Thailand. Foods 13:113. *https://doi.org/10.3390/foods13010113*

Saengha W, Karirat T, Buranrat B, Matra K, Deeseenthum S, Katisart T, Luang-In V (2021). Non-thermal plasma treatment on mustard green seeds and its effect on growth, isothiocyanates, antioxidant activity, and anticancer activity of microgreens. International Journal of Agriculture and Biology 25(3):667-676. *https://doi.org/10.17957/IJAB/15.1715*

Sarangapani C, Devi Y, Thirundas R, Annapure US, Deshmukh RR (2017). Effect of low-pressure plasma on physico-chemical properties of parboiled rice. LWT - Food Science and Technology 79:482-490. *https://doi.org/10.1016/j.lwt.2017.01.065*

Sarkar T, Salauddin M, Roy S, Chakraborty R, Rebezov M, Shariati MA, Thiruvengadam M, Rengasamy KRR (2023). Underutilized green leafy vegetables: Frontier in fortified food development and nutrition. Critical Reviews in Food Science and Nutrition 63(33):11679-11733. *https://doi.org/10.1080/10408398.2022.2095555*

Seeram NP, Schutzki R, Chandra A, Nair MG (2002). Characterization, quantification, and bioactivities of anthocyanins in Cornus species. Journal of Agricultural and Food Chemistry 50(9):2519-2523. *https://doi.org/10.1021/jf0115903*

Tanakaran Y, Matra K (2022). The Influence of atmospheric non-thermal plasma on jasmine rice seed enhancements. Journal of Plant Growth Regulation 41(1):178-187. *https://doi.org/10.1007/s00344-020-10275-1*

Traversari S, Pistelli L, Del Ministro B, Cacini S, Costamagna G, Ginepro M, Marchioni I, Orlandini A, Massa D (2021). Combined effect of silicon and non-thermal plasma treatments on yield, mineral content, and nutraceutical proprieties of edible flowers of *Begonia cucullata*. Plant Physiology and Biochemistry 166:1014-1021. *https://doi.org/10.1016/j.plaphy.2021.07.012*

Tunsagool P, Pimpak V, Promwat P, Kwandee P, Kruaweangmol P, Roytrakul S, Withayagiat U (2023). Metabolomic profiling of health-benefit compounds in fresh and preserved mustard greens. International Journal of Food Science and Technology 59(6):4290-4299. *https://doi.org/10.1111/ijfs.16865*

Verkerk R, Schreiner M, Krumbein A, Ciska E, Holst B, Rowland I, ... Dekker M (2009). Glucosinolates in Brassica vegetables: The influence of the food supply chain on intake, bioavailability, and human health. Molecular Nutrition and Food Research 53(Suppl 2):S219. *https://doi.org/10.1002/mnfr.200800065*

Wang L, Tian Z, Yang Q, Li H, Guan H, Shi B, et al. (2015). Sulforaphane inhibits thyroid cancer cell growth and invasiveness through the reactive oxygen species-dependent pathway. Oncotarget 6(28):25917-25931. *https://doi.org/10.18632/oncotarget.4542*

Wang Q, Li D, Liu L, Shan Y, Bao Y (2024). Dietary isothiocyanates and anticancer agents: Exploring synergism for improved cancer management. Frontiers in Nutrition 11:1386083. *https://doi.org/10.3389/fnut.2024.1386083*

Zeng W, Yang J, He Y, Zhu Z (2023). Bioactive compounds in cruciferous sprouts and microgreens and the effects of sulfur nutrition. Journal of the Science of Food and Agriculture 103(15):7323-7332. *https://doi.org/10.1002/jsfa.12755*